

# The Rate-Determining Step on the recA Protein-Catalyzed ssDNA-Dependent ATP Hydrolysis Reaction Pathway<sup>†</sup>

Einar Stole and Floyd R. Bryant\*

Department of Biochemistry, The Johns Hopkins University, School of Public Health, Baltimore, Maryland 21205

Received November 21, 1996; Revised Manuscript Received January 21, 1997<sup>®</sup>

**ABSTRACT:** We recently constructed a mutant recA protein in which His163 was replaced by a tryptophan residue. The [H163W]recA protein is functionally identical to the wild-type protein, and the Trp163 side chain serves as a fluorescence reporter group for the ATP and ATP $\gamma$ S-mediated conformational transitions of the [H163W]recA–ssDNA complex. In this report, the pre-steady-state kinetics of the ATP and ATP $\gamma$ S-mediated transitions were examined by stopped-flow fluorescence. The kinetics of the ATP-mediated fluorescence change were consistent with a two-step mechanism in which an initial rapid equilibrium binding of ATP to the recA–ssDNA complex is followed by a first-order isomerization of the complex to a new conformational state; the rate constant for the isomerization step of 18 min<sup>−1</sup> is identical to the steady-state turnover number for ATP hydrolysis. The kinetics of the ATP $\gamma$ S-mediated fluorescence change were also consistent with a two-step binding mechanism with a unimolecular isomerization of 18 min<sup>−1</sup>; since ATP $\gamma$ S is not hydrolyzed appreciably on the time scale of these experiments (0.017 min<sup>−1</sup>), this indicates that the isomerization step follows ATP $\gamma$ S (or ATP) binding but precedes ATP $\gamma$ S (or ATP) hydrolysis. These and other results are consistent with a kinetic model in which an ATP-mediated isomerization of the recA–ssDNA complex is the rate-determining step on the recA protein-catalyzed ssDNA-dependent ATP hydrolysis reaction pathway.

The recA protein of *Escherichia coli* ( $M_r$ , 37 842; 352 amino acids) is essential for homologous genetic recombination and for the postreplicative repair of damaged DNA. The purified recA protein promotes a variety of DNA pairing reactions that presumably reflect *in vivo* recombination functions. The most extensively investigated DNA pairing reaction is the ATP-dependent three-strand exchange reaction, in which a circular ssDNA<sup>1</sup> molecule and a homologous linear dsDNA molecule are recombined to yield a nicked circular dsDNA molecule and a linear ssDNA molecule. This reaction proceeds in three phases. In the first phase, the circular ssDNA substrate is coated with recA protein to form a presynaptic complex; this complex will catalyze the hydrolysis of ATP to ADP and P<sub>i</sub>. In the second phase, the presynaptic complex interacts with a dsDNA molecule, the homologous sequences are brought into register, and pairing between the circular ssDNA and the complementary strand from the dsDNA is initiated. In the third phase, the complementary linear strand is completely transferred to the circular ssDNA by unidirectional branch migration to yield the nicked circular dsDNA and displaced linear ssDNA products (Roca & Cox, 1990; Kowalczykowski, 1991).

The presynaptic complex formed between recA protein and ssDNA is the active recombinational entity in the strand exchange reaction. The recA protein binds cooperatively to ssDNA, forming a right-handed helical protein filament with 1 recA monomer/4 nucleotides of ssDNA and 6 recA

monomers/turn of the filament. In the absence of nucleotide cofactor or in the presence of ADP, the helical filament exists in a “collapsed” or “closed” conformation (helical pitch, 65 Å) that is inactive in strand exchange. In the presence of ATP, however, the filament isomerizes to an “extended” or “open” conformation (helical pitch, 95 Å) that is active in strand exchange. The filament also isomerizes to the open conformation and is active in strand exchange in the presence of the poorly hydrolyzed ATP analog, ATP $\gamma$ S, indicating that nucleotide hydrolysis is not required for either of these processes (Egelman, 1993).

In order to monitor the conformational transitions of the recA protein directly, we recently constructed a mutant recA protein in which His163 in the loop 1 region (residues 157–163) of the protein was replaced by a tryptophan reporter group. The [H163W]recA protein catalyzes ATP hydrolysis with the same turnover number as does the wild-type protein (18 min<sup>−1</sup>), has a  $S_{0.5}(\text{ATP})$  value (70  $\mu\text{M}$ ) that is similar to that of the wild-type protein (45  $\mu\text{M}$ ), and is fully functional in the three-strand exchange reaction.<sup>2</sup> In addition, the fluorescence of the Trp163 reporter group is very sensitive to the binding of nucleotide cofactors: ADP causes only a minor change in the fluorescence of the [H163W]recA–ssDNA complex (closed conformation), whereas ATP and ATP $\gamma$ S lead to a more substantial change in the fluorescence of the complex (open conformation). These results demonstrated that the conformational state of the [H163W]recA–ssDNA complex could be monitored by following the fluorescence of the Trp163 reporter group (Stole & Bryant, 1994, 1995). In this report, we examine the kinetics of the nucleotide cofactor-mediated fluorescence changes of the [H163W]recA–ssDNA complex by stopped-flow fluores-

<sup>†</sup> This work was supported by grant RO1 GM 36516 (F. R. B.) and postdoctoral grant F32 GM16284 (E. S.) from the National Institutes of Health.

\* Author to whom correspondence should be addressed.

<sup>®</sup> Abstract published in *Advance ACS Abstracts*, March 15, 1997.

<sup>1</sup> Abbreviations: ssDNA, single-stranded DNA; dsDNA, double-stranded DNA;  $\phi$ X, bacteriophage  $\phi$ X174; ATP $\gamma$ S, adenosine 5'-O-(thiotriphosphate).

<sup>2</sup>  $S_{0.5}$  is the substrate concentration required for half-maximal velocity.

cence in order to elucidate the elementary steps on the recA protein-catalyzed ssDNA-dependent ATP hydrolysis reaction pathway.

## EXPERIMENTAL PROCEDURES

### Materials

Wild-type and [H163W]recA protein were prepared as described previously (Bryant, 1988; Stole & Bryant, 1994). ATP, ADP, and ATP $\gamma$ S were from Sigma. [ $\alpha$ - $^{32}$ P]ATP and [ $\gamma$ - $^{32}$ P]ATP were from ICN. [8- $^{14}$ C]ATP $\gamma$ S was prepared from [8- $^{14}$ C]ADP using ATP $\gamma$ S and nucleoside diphosphate kinase (Sigma) as described previously (Menge & Bryant, 1992). Oligo dT<sub>50</sub> DNA was from the DNA oligonucleotide synthesis facility at Johns Hopkins University, and circular  $\phi$ X ssDNA ((+)strand) was prepared as described previously (Cox & Lehman, 1981). All DNA concentrations are expressed as total nucleotides.

### Fluorescence Analysis

Steady-state fluorescence measurements were made with a SLM Aminco-Bowman Series 2 luminescence spectrometer equipped with a variable-temperature holder. The concentrations of stock solutions of the purified wild-type and [H163W]recA proteins were determined by absorbance using the extinction coefficients 0.59 and 1.2 A<sub>280</sub> mg<sup>-1</sup> mL, respectively (Stole & Bryant, 1994). Each fluorescence emission spectrum was corrected for background fluorescence by subtracting the corresponding buffer spectrum.

Stopped-flow fluorescence time courses were obtained with the SLM Aminco-Bowman Series 2 luminescence spectrometer using a MilliFlow stopped-flow reactor. The emission wavelength was 345 nm (emission monochromator), and the excitation wavelength was 295 nm. The excitation and emission bandwidths were 4 nm, and the estimated dead time for the instrument was 2–3 ms. Least-squares fitting of the data was accomplished using the curve-fitting program Enzfitter (Biosoft).

## RESULTS

### Steady-State Kinetics of Oligo dT<sub>50</sub>-Dependent ATP Hydrolysis

The steady-state kinetic parameters for ssDNA-dependent ATP hydrolysis by the [H163W]recA protein were determined previously using  $\phi$ X ssDNA (5386 nucleotides) as the ssDNA effector (Stole & Bryant, 1994, 1995). For the stopped-flow fluorescence measurements described in this report, we chose to use the smaller oligomer, dT<sub>50</sub>, as the ssDNA effector (oligo dT<sub>50</sub> is the smallest ssDNA that will maximally activate the ATP hydrolysis activity of the wild-type recA protein (Brenner et al., 1987)). The steady-state kinetic parameters for the oligo dT<sub>50</sub>-dependent ATP hydrolysis reaction were determined at pH 7.5 and 37 °C with 1  $\mu$ M [H163W]recA protein and 10  $\mu$ M oligo dT<sub>50</sub> (standard reactions conditions).

As shown in Figure 1, the turnover number ( $V_{\max}/[E_T]$ ) for the oligo dT<sub>50</sub>-dependent ATP hydrolysis reaction was 18 min<sup>-1</sup> and the  $S_{0.5}(\text{ATP})$  was 70  $\mu$ M. Furthermore, the ATP saturation curve was sigmoidal, indicating that the ATP hydrolysis reaction is subject to positive cooperativity with respect to ATP concentration, with a Hill coefficient ( $n$ ) of

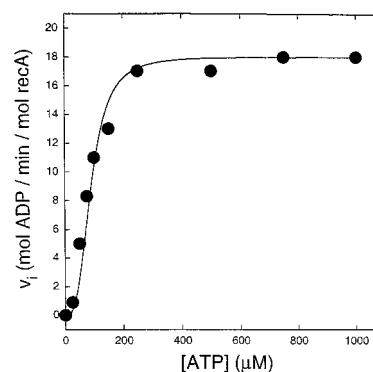


FIGURE 1: Oligo dT<sub>50</sub>-dependent ATP hydrolysis by the [H163W]-recA protein. The reaction solutions contained 25 mM Tris-HCl (pH 7.5), 10 mM MgCl<sub>2</sub>, 10  $\mu$ M oligo dT<sub>50</sub>, 1.0  $\mu$ M [H163W]-recA protein, 1 mM DTT, 5% glycerol, and the indicated concentration of [ $\gamma$ - $^{32}$ P]ATP. The reactions were initiated by addition of enzyme and were carried out at 37 °C. ATP hydrolysis was measured by a thin layer chromatography method as described previously (Weinstock et al., 1979). The points represent the initial rates of ATP hydrolysis measured at the indicated concentrations of ATP. Each point is based on the average of four independent determinations; the error range for each point was less than  $\pm 10\%$ , except for 25  $\mu$ M ATP which was  $\pm 20\%$ . The solid line was calculated using the standard Hill equation and the parameters  $V_{\max}/[E_T] = 18 \text{ min}^{-1}$ ,  $S_{0.5} = 70 \mu\text{M}$ , and  $n = 3$ .

3. These values are identical to those obtained previously with  $\phi$ X ssDNA (Stole & Bryant, 1994, 1995).

### Steady-State Fluorescence Properties of the [H163W]recA-Oligo T<sub>50</sub> Complex

The effects of nucleotide cofactors on the steady-state tryptophan fluorescence of the [H163W]recA–ssDNA complex were previously determined using  $\phi$ X ssDNA as the ssDNA effector (Stole & Bryant, 1994, 1995). These fluorescence measurements were made by adding a small aliquot of the nucleotide cofactor (1% of total volume) to a solution containing preformed [H163W]recA–ssDNA complex; this procedure was employed to minimize dilution effects occurring upon addition of the nucleotide cofactor (aliquot mixing method). For the present study, we remeasured the effects of nucleotides on the steady-state fluorescence of the [H163W]recA–ssDNA complex using oligo dT<sub>50</sub> as the ssDNA effector so that we could directly correlate the steady-state fluorescence changes with the pre-steady-state fluorescence changes that were measured by stopped-flow fluorescence (see below). In addition, in order to duplicate the mixing conditions of the stopped-flow measurements, the new steady-state fluorescence measurements were made by mixing a solution containing the [H163W]-recA–ssDNA complex with an equal volume of buffer solution containing the nucleotide cofactor (stopped-flow mixing method). The excitation wavelength was 295 nm, and emission intensity was measured at the emission maximum of 345 nm (Stole & Bryant, 1995). All measurements were made under standard reaction conditions.

As shown in Table 1, the addition of ADP (1 mM) resulted in no change in the tryptophan fluorescence of the [H163W]-recA–ssDNA complex. This is consistent with the observation that the conformation of the recA–ssDNA complex in the presence of ADP is similar (as judged by electron microscopy) to that in the absence of nucleotide cofactor (Egelman, 1993). In contrast, the addition of ATP (1 mM) resulted in a 10% decrease in total fluorescence (correspond-

Table 1: Effect of Nucleotide Cofactors on the Tryptophan Fluorescence of Wild-Type and [H163W]recA–ssDNA Complexes. Stopped-Flow Conditions<sup>a</sup>

complex	% $\Delta F_{\text{total}}$	% $\Delta F_{\text{W163}}$
wild-type recA		
+ ADP	1	
+ ATP	1	
+ ATP $\gamma$ S	1	
[H163W]recA		
+ ADP	1	2
+ ATP	10	25
+ ATP $\gamma$ S	13	33

<sup>a</sup> A solution containing 2  $\mu\text{M}$  [H163W]recA protein and 20  $\mu\text{M}$  oligo dT<sub>50</sub> in reaction buffer (25 mM Tris-HCl (pH 7.5), 10 mM MgCl<sub>2</sub>, 1 mM DTT, and 5% glycerol) was mixed with an equal volume of a solution containing either reaction buffer alone or reaction buffer plus 2 mM of the indicated nucleotide. Fluorescence emission spectra were then recorded at 37.0  $\pm$  0.1  $^{\circ}\text{C}$ . The excitation wavelength was 295 nm, and emission was measured at 345 nm. The excitation and emission bandwidths were set at 5 nm. The total fluorescence change (%  $\Delta F_{\text{total}}$ ) is defined as  $(I_0 - I)/I_0$ , where  $I_0$  is the fluorescence intensity measured after addition of buffer alone and  $I$  is the intensity measured after addition of the indicated nucleotide cofactor. Since the fluorescence intensity of the [H163W]recA protein is 68% greater than that of the wild-type protein, the change in Trp163 fluorescence (%  $\Delta F_{\text{W163}}$ ) was calculated using the relationship %  $\Delta F_{\text{W163}} = 2.68\Delta F_{\text{H163W}} - 1.68\Delta F_{\text{WT}}$ , where  $\Delta F_{\text{H163W}}$  and  $\Delta F_{\text{WT}}$  are the total fluorescence changes observed for the mutant and wild-type recA proteins, respectively, under a specified set of conditions. This calculation assumes that the fluorescence properties of the intrinsic tryptophans (Trp290 and Trp308) are not affected by the introduction of a tryptophan residue at position 163 of the recA protein (Stole & Bryant, 1994).

ing to a 25% decrease in the fluorescence of the Trp163 reporter group). The observation of a fluorescence change with ATP is consistent with the ATP-mediated isomerization of the [H163W]recA–ssDNA complex from the closed to the open conformation. Similarly, the addition of ATP $\gamma$ S resulted in a 13% decrease in total fluorescence (corresponding to a 33% decrease in Trp163 fluorescence), consistent with the ATP $\gamma$ S-mediated isomerization of the complex from the closed to the open conformation. Since it has been shown that the recA–ssDNA complex at saturation binds 1 molecule of ATP $\gamma$ S/recA monomer (Weinstock et al., 1981), the steady-state fluorescence changes reported in Table 1 presumably correspond to the complete conversion of all of the [H163W]recA monomers within the [H163W]recA–ssDNA complex to the nucleotide-bound state. As found previously with  $\phi\text{X}$  ssDNA (Stole & Bryant, 1994, 1995), none of the nucleotides had an appreciable effect on the fluorescence of the wild-type recA–oligo dT<sub>50</sub> complex under these conditions (Table 1).<sup>3</sup>

Although the relative effects of the different nucleotides on the steady-state fluorescence of the [H163W]recA–ssDNA complex are similar to those measured before, the magnitudes of the fluorescence changes reported here under stopped-flow mixing conditions are somewhat different than those obtained previously by the aliquot mixing method (Stole & Bryant, 1994, 1995). This indicates that the observed magnitudes are dependent on the exact mixing conditions, possibly due to differences in the higher order

<sup>3</sup> The wild-type recA protein has two intrinsic tryptophan residues (Trp290 and Trp308), both of which are located in a small carboxy-terminal domain (amino acids 270–352) that protrudes from the surface of the recA protein filament (Story et al., 1992). This domain may not be affected appreciably by conformational changes of the recA–ssDNA complex.

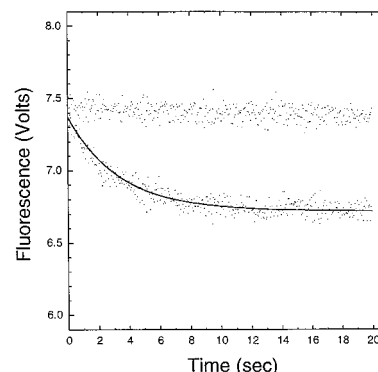


FIGURE 2: Pre-steady-state time course of the ATP-mediated change in the fluorescence of the [H163W]recA–ssDNA complex. A solution containing 2  $\mu\text{M}$  [H163W]recA protein and 20  $\mu\text{M}$  oligo dT<sub>50</sub> in reaction buffer (25 mM Tris-HCl (pH 7.5), 10 mM MgCl<sub>2</sub>, 1 mM DTT, and 5% glycerol) was mixed with an equal volume of solution consisting of either reaction buffer alone (upper time course) or reaction buffer plus 2 mM ATP (lower time course). The data points represent the fluorescence emission of the resulting solutions as measured at 345 nm (excitation wavelength = 295 nm) at the indicated times after mixing. The solid line represents a least-squares fit of the data by a single exponential with a first-order rate constant of 18 min<sup>−1</sup>.

aggregation states of the [H163W]recA–ssDNA complexes. The method of mixing, however, has no effect on the observed rate of ssDNA-dependent ATP hydrolysis (or, therefore, on the amount of [H163W]recA protein bound to ssDNA) (data not shown).

#### Stopped-Flow Fluorescence

The pre-steady-state time courses of the nucleotide-mediated changes in the fluorescence of the [H163W]recA–ssDNA complex were examined by stopped-flow fluorescence. All measurements were made under standard reaction conditions by mixing a solution containing the [H163W]recA–ssDNA complex from one syringe with an equal volume of a solution containing the nucleotide cofactor from the second syringe (final concentration: 1  $\mu\text{M}$  [H163W]recA protein and 10  $\mu\text{M}$  oligo dT<sub>50</sub>). The excitation wavelength was 295 nm, and fluorescence intensity was monitored at 345 nm.

**ADP.** When a saturating concentration of ADP (1 mM) was mixed with the [H163W]recA–ssDNA complex, there was no indication of a rapid or transient change in the fluorescence of the Trp163 reporter group (data not shown). This result is consistent with the absence of a change in the steady-state fluorescence of the [H163W]recA–ssDNA complex that was observed when ADP was added under stopped-flow mixing conditions (Table 1).

**ATP.** The pre-steady-state time course of the ATP-mediated change in the fluorescence of the [H163W]recA–ssDNA complex that was obtained at a saturating concentration of ATP (1 mM) is shown in Figure 2. The time course of the fluorescence change followed a single exponential with a first-order rate constant of 18 min<sup>−1</sup>. The amplitude of the fluorescence change (10%) was identical to the change in the steady-state fluorescence of the [H163W]recA–ssDNA complex that was measured with 1 mM ATP under stopped-flow mixing conditions (Table 1). There was no change in fluorescence when the [H163W]recA–ssDNA complex was mixed with buffer alone (Figure 2).

The time course of the ATP-mediated fluorescence change was also measured over a range of ATP concentrations (50–

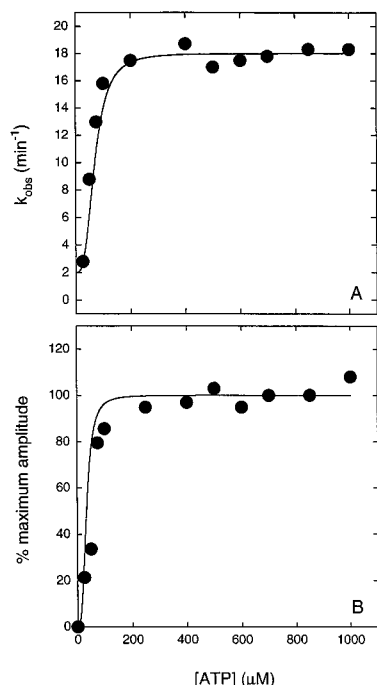
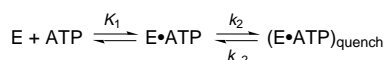


FIGURE 3: Dependence of the ATP-mediated fluorescence change on ATP concentration. The time course of the ATP-mediated change in the fluorescence of the [H163W]recA–ssDNA complex was measured over a range of ATP concentrations (50–1000  $\mu\text{M}$ ). Fluorescence measurements were made as described in the legend to Figure 2. Each of the transient fluorescence time courses was fitted by a single exponential decay. Panel A. Dependence of the observed first-order rate constant of the ATP-mediated fluorescence change on ATP concentration. The data points represent the observed first-order rate constants that were determined at the indicated concentrations of ATP. The solid line was calculated using the modified two-step binding mechanism described in the text (equation 2) and the parameters  $k_2 = 16 \text{ min}^{-1}$ ,  $k_{-2} = 2 \text{ min}^{-1}$ ,  $S_{0.5} = 70 \text{ }\mu\text{M}$ , and  $n = 3$ . Panel B. Dependence of the amplitude of the ATP-mediated fluorescence change on ATP concentration. The data points represent the amplitudes of the fluorescence changes that were obtained at the indicated concentrations of ATP. Each point is based on the average of four independent determinations; the error range for each point was less than  $\pm 10\%$ , except for 25  $\mu\text{M}$  ATP which was  $\pm 25\%$ . The solid line was calculated using the modified two-step binding mechanism described in the text (eq 3) and the parameters given above for Figure 3A.

1000  $\mu\text{M}$ ). In all cases, the time courses followed a single exponential. The dependence of the observed first-order rate constant for the fluorescence change on ATP concentration is shown in Figure 3A, and the dependence of the amplitude of the fluorescence change on ATP concentration is shown in Figure 3B.

As shown in Figure 3A, the observed rate constant for the fluorescence change increased with increasing ATP concentration until reaching a maximum value of  $18 \text{ min}^{-1}$  at ATP concentrations greater than approximately 200  $\mu\text{M}$ . These results could be approximated by a simple two-step binding mechanism (Scheme 1) in which ATP binds to the recA–ssDNA complex (designated E) in a rapid equilibrium step (association constant  $K_1$ ), which is followed by a first-order isomerization of the complex to a new conformational (quenched fluorescence) state with a rate constant of  $18 \text{ min}^{-1}$ .

#### Scheme 1

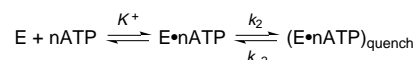


In this mechanism, the dependence of the observed first-order rate constant ( $k_{\text{obs}}$ ) for the fluorescence change on ATP concentration is given by

$$k_{\text{obs}} = k_2(K_1[\text{ATP}]/1 + K_1[\text{ATP}]) + k_{-2} \quad (1)$$

where  $k_2$  represents the intrinsic first-order rate constant for the isomerization step,  $k_{-2}$  is the rate constant for the reversal of the isomerization, and  $(K_1[\text{ATP}]/1 + K_1[\text{ATP}])$  corresponds to the fractional saturation of the recA–ssDNA complex with ATP. Although the fit of eq 1 to the data was satisfactory (fit not shown), a better fit was obtained using a modified two-step binding mechanism (Scheme 2), which accounts for the cooperative binding of ATP to the recA–ssDNA complex

#### Scheme 2



In this mechanism, the dependence of the observed first-order rate constant for the fluorescence change on ATP concentration is given by

$$k_{\text{obs}} = k_2(K^+[\text{ATP}]^n/1 + K^+[\text{ATP}]^n) + k_{-2} \quad (2)$$

In this equation, the fractional saturation term has been replaced by the Hill expression for cooperative binding (where  $K^+ = 1/[S_{0.5}]^n$ ). The parameters obtained from the fit of eq 2 to the data in Figure 3A were  $k_{\text{obs}}(\text{max}) = 18 \text{ min}^{-1}$ ,  $S_{0.5} = 70 \text{ }\mu\text{M}$ , and  $n = 3$ . These values are identical to the values for the turnover number ( $18 \text{ min}^{-1}$ ),  $S_{0.5}$  (70  $\mu\text{M}$ ), and  $n$  (3) that were obtained from the steady-state kinetics of the ssDNA-dependent ATP hydrolysis reaction under these same conditions (Figure 1). The data in Figure 3A do not allow a unique value for  $k_{-2}$  to be assigned ( $k_{-2}$  is given by the intercept on the y-axis) and can be fit with values of  $k_{-2}$  ranging from 0 to  $2 \text{ min}^{-1}$ . The fit shown in Figure 3A was generated using  $k_2 = 16 \text{ min}^{-1}$  and  $k_{-2} = 2 \text{ min}^{-1}$  ( $k_{\text{obs}}(\text{max}) = k_2 + k_{-2}$ ); these values were derived from the dependence of the fluorescence amplitude on ATP concentration as described below.

As shown in Figure 3B, the amplitude of the fluorescence change varied with ATP concentration, reaching a maximum value at ATP concentrations greater than approximately 200  $\mu\text{M}$ . For the modified two-step binding mechanism shown in Scheme 2, the amplitude is determined by the relative steady-state concentration of the quenched complex,  $[(\text{E} \cdot \text{ATP})_{\text{q}}]/[\text{E}_{\text{tot}}]$ , and the dependence of the amplitude on ATP concentration is given by

$$[(\text{E} \cdot \text{ATP})_{\text{q}}]/[\text{E}_{\text{tot}}] = K^+K_2[\text{ATP}]^n/1 + K^+K_2[\text{ATP}]^n + K^+K_2[\text{ATP}]^n \quad (3)$$

where  $K^+ = 1/[S_{0.5}]^n$  and  $K_2 = k_2/k_{-2}$ . The data shown in Figure 3B can be fit by eq 3 with the parameters  $S_{0.5} = 70 \text{ }\mu\text{M}$ ,  $k_2 = 16 \text{ min}^{-1}$ , and  $k_{-2} = 2 \text{ min}^{-1}$ . These parameters are identical to those that were used to fit the ATP concentration dependence of the observed rate constant for the fluorescence change to this same mechanism in Figure 3A. The fact that the same kinetic parameters can describe the ATP concentration dependence of both the observed rate constant and the amplitude of the fluorescence change

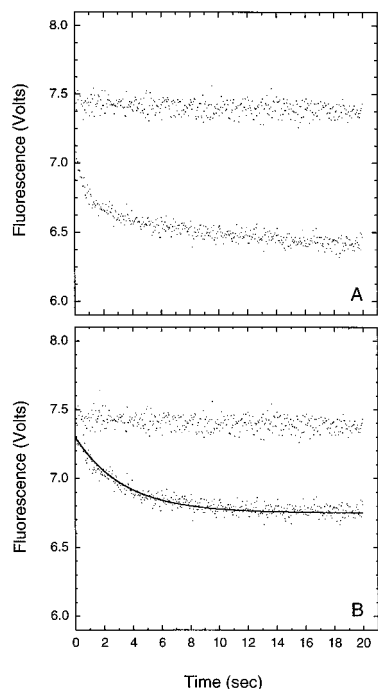


FIGURE 4: Pre-steady-state time course of the ATP $\gamma$ S-mediated change in the fluorescence of the [H163W]recA-ssDNA complex. A solution containing 2  $\mu$ M [H163W]recA protein and 20  $\mu$ M oligo dT<sub>50</sub> in reaction buffer (25 mM Tris-HCl (pH 7.5), 10 mM MgCl<sub>2</sub>, 1 mM DTT, and 5% glycerol) was mixed with an equal volume of solution consisting of either reaction buffer alone (upper time course) or reaction buffer plus 2 mM ATP $\gamma$ S (lower time course). The data points represent the fluorescence of the resulting solutions as measured at 345 nm (excitation wavelength = 295 nm) at the indicated times after mixing. Panel A. Time course of the total fluorescence change. Panel B. Time course of the major phase of the fluorescence change. In this plot, the initial rapid component of the fluorescence change was subtracted from the total change in fluorescence; this component corresponded to approximately 20% of the total decrease in fluorescence and was independent of ATP $\gamma$ S concentration. The solid line represents a least-squares fit of the corrected data by a single exponential with a first-order rate constant of 18 min<sup>-1</sup>.

indicates that the mechanism in Scheme 2 is sufficient at least to a first approximation to account for the pre-steady-state interactions between the recA-ssDNA complex and ATP.

**ATP $\gamma$ S.** The pre-steady-state time course of the ATP $\gamma$ S-mediated change in the fluorescence of the [H163W]recA-ssDNA complex that was obtained at a saturating concentration of ATP $\gamma$ S (1 mM) is shown in Figure 4. The time course was similar to that obtained with ATP, except that there was an initial rapid decrease in fluorescence which accounted for approximately 20% of the total fluorescence change. This initial decrease was followed by a much larger first-order fluorescence change that was identical both in rate and in amplitude to that observed with ATP. The initial decrease in fluorescence accounts for the slightly higher total change in steady-state fluorescence that was observed with ATP $\gamma$ S relative to that with ATP (Table I). The time course of the total fluorescence change is shown in Figure 4A, and the time course of the major phase of the fluorescence change (obtained by subtracting the initial decrease from the total fluorescence time course) is shown in Figure 4B.

The time course of the ATP $\gamma$ S-mediated fluorescence change was also measured over a range of ATP $\gamma$ S concentrations (50–1000  $\mu$ M). The rate and amplitude of the initial

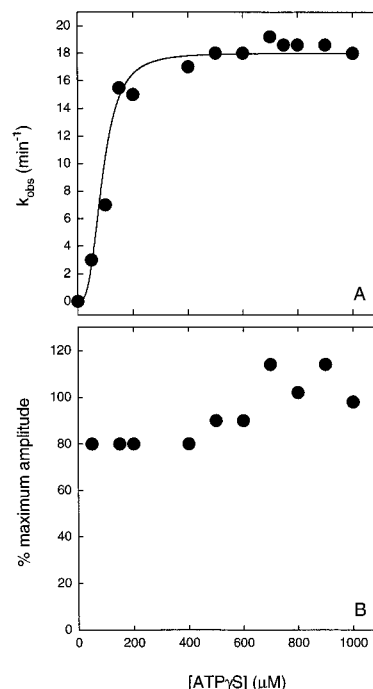


FIGURE 5: Dependence of the ATP $\gamma$ S-mediated fluorescence change on ATP $\gamma$ S concentration. The time course of the ATP $\gamma$ S-mediated change in the fluorescence of the [H163W]recA-ssDNA complex was measured over a range of ATP $\gamma$ S concentrations (50–1000  $\mu$ M). Fluorescence measurements were made as described in the legend to Figure 4. Each of the transient fluorescence time courses was fitted by a single exponential decay. Panel A. Dependence of the observed first-order rate constant of the ATP $\gamma$ S-mediated fluorescence change on ATP $\gamma$ S concentration. The data points represent the observed first-order rate constants that were determined at the indicated concentrations of ATP $\gamma$ S. The solid line was calculated using the modified two-step binding mechanism described in the text (eq 4) and the parameters  $k_2 = 18$  min<sup>-1</sup>,  $k_{-2} = 0$ ,  $S_{0.5} = 90$   $\mu$ M, and  $n = 3$ . Panel B. Dependence of the amplitude of the ATP $\gamma$ S-mediated fluorescence change on ATP $\gamma$ S concentration. The data points represent the amplitudes of the fluorescence changes that were obtained at the indicated concentrations of ATP $\gamma$ S.

minor decrease in fluorescence were independent of ATP $\gamma$ S concentration over the concentration range examined (data not shown); the origin of the initial decrease (including the possibility that it arises from the binding of ATP $\gamma$ S to a subset of high-affinity binding sites within the polymeric recA-ssDNA complex) is under investigation. In contrast, the time courses for the major phase of the fluorescence change all followed a single exponential which depended directly on ATP $\gamma$ S concentration. The dependence of the observed first-order rate constant for the major fluorescence change on ATP $\gamma$ S concentration is shown in Figure 5A, and the dependence of the amplitude of the major fluorescence change on ATP $\gamma$ S concentration is shown in Figure 5B.

As shown in Figure 5A, the observed rate constant for the major fluorescence change increased with increasing ATP $\gamma$ S concentration until reaching a maximum value of 18 min<sup>-1</sup> at ATP $\gamma$ S concentrations greater than approximately 200  $\mu$ M. These results are consistent with the modified two-step binding mechanism (Scheme 3), in which ATP $\gamma$ S binds cooperatively to the recA-ssDNA complex (E) in a rapid equilibrium step, which is followed by a first-order isomerization of the complex to a new conformational (quenched fluorescence) state with a rate constant of 18 min<sup>-1</sup>.

## Scheme 3



As before, the dependence of the observed first-order rate constant for the fluorescence change on ATP $\gamma$ S concentration is given by

$$k_{\text{obs}} = k_2(K^+[\text{ATP}\gamma\text{S}]^n/1 + K^+[\text{ATP}\gamma\text{S}]^n) + k_{-2} \quad (4)$$

The parameters obtained from the fit of eq 4 to the data in Figure 5A were  $k_{\text{obs}}(\text{max}) = 18 \text{ min}^{-1}$ ,  $S_{0.5} = 90 \mu\text{M}$ , and  $n = 3$ . Notably, the rate of the proposed first-order isomerization of the [H163W]recA–ssDNA complex with ATP $\gamma$ S is identical to that obtained with ATP and identical to the rate of ssDNA-dependent ATP hydrolysis under these conditions. The data do not allow a unique value of  $k_{-2}$  to be assigned and can be fit with values of  $k_{-2}$  ranging from 0 to  $2 \text{ min}^{-1}$ . The fit shown in Figure 5A was generated using values of  $k_2 = 18 \text{ min}^{-1}$  and  $k_{-2} = 0$ . The selection of a zero value for  $k_{-2}$  was based on the low reversibility of the isomerization step with ATP $\gamma$ S, as indicated by the independence of the fluorescence amplitude on ATP $\gamma$ S concentration described below.<sup>4</sup>

As shown in Figure 5B, the amplitude of the ATP $\gamma$ S-mediated fluorescence change was roughly independent of ATP $\gamma$ S concentration over the range of ATP $\gamma$ S concentrations examined. This is in contrast to the saturation behavior observed with ATP (Figure 3B) and indicates that the ATP $\gamma$ S-induced isomerization of the [H163W]recA–ssDNA complex may be only weakly reversible over the concentration range examined. This is likely due to the fact that, in contrast to ATP, ATP $\gamma$ S is only slowly hydrolyzed by the recA protein (see below).

#### Pre-Steady-State Time Courses of ATP and ATP $\gamma$ S Hydrolysis

The pre-steady-state time courses for the [H163W]recA protein-catalyzed ssDNA-dependent ATP and ATP $\gamma$ S hydrolysis reactions are shown in Figure 6. These time courses were obtained under stopped-flow reaction conditions in which a solution containing the [H163W]recA–ssDNA complex was mixed with an equal volume of a solution containing a saturating concentration of either ATP $\gamma$ S or ATP. Reactions were carried out both with the standard concentration ( $1 \mu\text{M}$ ) and with higher concentrations of [H163W]recA protein ( $5\text{--}10 \mu\text{M}$ ) in order to ensure that the first turnover of nucleotide hydrolysis could be measured accurately.

The time course of the ATP $\gamma$ S hydrolysis reaction is shown in Figure 6A. The reaction, which was monitored both by the release of ADP (Figure 6A) and by the release of thiophosphate (not shown), followed a linear time course with a steady-state rate constant of  $0.017 \text{ min}^{-1}$ , with no indication of a rapid hydrolysis of a single equivalent of ATP $\gamma$ S during the pre-steady-state phase of the reaction.<sup>5</sup> The absence of a burst of ATP $\gamma$ S hydrolysis indicates that the reaction does not proceed by the rapid hydrolysis of a

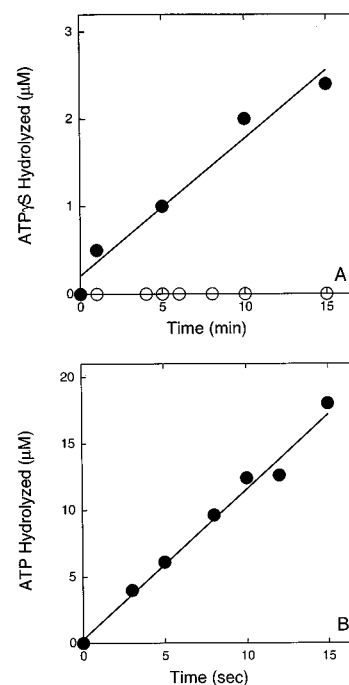


FIGURE 6: Pre-steady-state time course of ssDNA-dependent ATP and ATP $\gamma$ S hydrolysis by the [H163W]recA protein. Panel A. ATP $\gamma$ S hydrolysis. A solution containing either  $2 \mu\text{M}$  [H163W]recA protein and  $20 \mu\text{M}$  oligo dT<sub>50</sub> (open circles), or  $20 \mu\text{M}$  [H163W]recA protein and  $200 \mu\text{M}$  oligo dT<sub>50</sub> (closed circles), in reaction buffer was mixed with an equal volume of a solution containing  $1 \text{ mM}$  [8-<sup>14</sup>C]ATP $\gamma$ S in reaction buffer. At the indicated times, aliquots were removed and the production of [8-<sup>14</sup>C]ADP was measured by PEI-cellulose thin layer chromatography using  $1 \text{ M}$  formic acid/ $0.5 \text{ M}$  LiCl as the mobile phase (Weinstock et al., 1979). It was presumed that the acidic mobile phase (pH 1.5) would denature the recA protein and release any protein-bound [8-<sup>14</sup>C]ADP into solution; similar results were obtained when reaction aliquots were quenched directly into  $1 \text{ M}$  formic acid before spotting on the thin layer plates. The data points represent the amount of [8-<sup>14</sup>C]ATP $\gamma$ S hydrolyzed as a function of time. Panel B. ATP hydrolysis. A solution containing  $10 \mu\text{M}$  [H163W]recA protein and  $100 \mu\text{M}$  oligo dT<sub>50</sub> in reaction buffer was mixed with an equal volume of a solution containing  $1 \text{ mM}$  [ $\alpha$ -<sup>32</sup>P]ATP in reaction buffer. At the indicated times, aliquots were removed, the reaction was quenched by the addition of an equal volume of EDTA ( $0.5 \text{ M}$ , pH 8.0), and the production of [ $\alpha$ -<sup>32</sup>P]ADP was measured by thin layer chromatography as described above. The data points represent the amount of [ $\alpha$ -<sup>32</sup>P]ATP hydrolyzed as a function of time.

single equivalent of ATP $\gamma$ S followed by a rate-determining release of either thiophosphate or ADP from the enzyme. Since the rate constant for ATP $\gamma$ S hydrolysis ( $0.017 \text{ min}^{-1}$ ) is 1000-fold lower than the rate constant for the ATP $\gamma$ S-mediated fluorescence change of  $18 \text{ min}^{-1}$  (Figure 5A), it is evident that the fluorescence change must be linked to a first-order isomerization step which follows ATP $\gamma$ S binding but precedes a slow ATP $\gamma$ S hydrolysis step.

The time course of the ATP hydrolysis reaction is shown in Figure 6B. The reaction followed a linear time course with a steady-state rate constant of  $18 \text{ min}^{-1}$ , with no indication of a burst of ATP hydrolysis during the first turnover. This result supports the idea that the rate-determining step of  $18 \text{ min}^{-1}$  occurs at or before the ATP hydrolysis step.

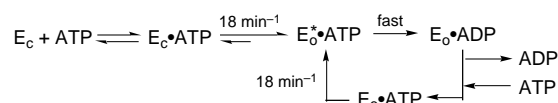
## DISCUSSION

The stopped-flow fluorescence and pre-steady-state kinetic results reported here are consistent with Scheme 4, where

<sup>4</sup> Independent measurements indicate that the  $k_{-2}$  value for ATP $\gamma$ S is  $\leq 0.13 \text{ min}^{-1}$  (Paulus, B., & Bryant, R., in preparation).

<sup>5</sup> The observed rate of ATP $\gamma$ S hydrolysis is similar to rates reported previously by others [see Yu and Egelman (1992)].

Scheme 4



$E_c$  represents the free recA–ssDNA complex in the initial unquenched fluorescence state (closed conformation),  $E_o$  represents the recA–ssDNA complex in the quenched fluorescence state (open conformation), and  $E_o^*$  represents the recA–ssDNA complex that has undergone ATP-mediated isomerization and is ready for ATP hydrolysis.

Scheme 4 begins with the first encounter between the free recA–ssDNA complex and ATP. The free recA–ssDNA complex is in the closed conformation and ATP binds to this complex in a rapid equilibrium step. This ATP binding step is followed by a first-order isomerization of the complex with a rate constant of  $18 \text{ min}^{-1}$ . Because this rate constant is identical to the turnover number for ATP hydrolysis, the pre-ATP hydrolysis isomerization step is presumed to be the rate-determining step on the ssDNA-dependent ATP hydrolysis reaction pathway. Thus, we propose that this  $18 \text{ min}^{-1}$  pre-ATP hydrolysis isomerization step must occur before every ATP hydrolysis event and have included it in Scheme 4 both for the approach to steady-state hydrolysis and in the steady-state cycle of ATP hydrolysis. During the first ATP binding sequence, the pre-ATP hydrolysis isomerization step is either accompanied by, or rapidly followed by (these alternatives are not distinguishable by our kinetic data) a conversion of the recA–ssDNA complex from the closed to the open conformation, as signaled by the change in the fluorescence of the complex from the unquenched to quenched state. Following the pre-ATP hydrolysis isomerization step, the first equivalent of ATP is hydrolyzed rapidly (relative to the rate-determining isomerization step) to ADP and  $P_i$ , thus, accounting for the absence of a burst of ADP or  $P_i$  production during the first turnover of ATP hydrolysis. The release of ADP and  $P_i$  and the binding of a new molecule of ATP to the recA–ssDNA complex must also be rapid, relative to the pre-ATP hydrolysis isomerization step (for simplicity,  $P_i$  has not been incorporated into Scheme 4).

The near equivalence of the steady-state fluorescence of the recA–ssDNA complex in the presence of either ATP or ATP $\gamma$ S indicates that the recA–ssDNA complex during steady-state ATP hydrolysis is in a state that closely resembles the fully open conformational state that is attained with the poorly hydrolyzed ATP analog, ATP $\gamma$ S. Since the dominant state during steady-state ATP hydrolysis (according to Scheme 4) will be the E·ATP complex that accumulates before the rate-determining pre-ATP hydrolysis isomerization step, it follows that this state must be in the quenched fluorescence state and therefore in the open conformation. This implies that although the transition of the recA–ssDNA complex from the closed to open state is dependent on the pre-ATP hydrolysis isomerization step during the approach to steady-state ATP hydrolysis, the closed to open transition may not occur during subsequent ATP hydrolysis events. That is, the pre-ATP hydrolysis isomerization step may be required for the closed to open transition, but is not coupled to it.

If the steady-state E•ATP complex that is reached by the release of the ADP and  $P_i$  hydrolysis products and the binding of a new ATP molecule is in the open conformation

(quenched fluorescence state), it follows that the E·ADP (or E·ADP·P<sub>i</sub>) complex that is formed during ATP hydrolysis will also be in the open conformation state. Even though the E·ADP (or E·ADP·P<sub>i</sub>) state will not be very populated during steady-state hydrolysis (the most populated state in Scheme 4 will be the E<sub>o</sub>·ATP state that accumulates before the rate-determining pre-ATP hydrolysis step), if it were to decay to the closed conformation, the subsequent E·ATP complex formed by the release of ADP and binding of a new ATP molecule would have to reisomerize to the open conformation in a rapid step before passing through the 18 min<sup>-1</sup> pre-ATP hydrolysis isomerization step a second time. Thus, if it is assumed that the pre-ATP hydrolysis isomerization step (18 min<sup>-1</sup>) is required for the closed to open transition, the results indicate that the E·ADP (or E·ADP·P<sub>i</sub>) complex that is reached via the ATP hydrolysis cycle is not equivalent to the E·ADP (or E·ADP·P<sub>i</sub>) complex that is formed when ADP (or ADP plus P<sub>i</sub>) is added directly to the free recA—ssDNA closed complex. The essential difference may be that when ADP is added directly to the free recA—ssDNA complex the complex will be filled entirely with ADP molecules which stabilize the closed conformation (unquenched fluorescence state), whereas during steady-state ATP hydrolysis the recA monomers which are bound to ADP molecules generated by the ATP hydrolysis reaction will be stabilized allosterically in the open conformation (quenched fluorescence state) by unhydrolyzed ATP molecules bound to adjacent recA monomers within the polymeric recA—ssDNA complex [see Lee and Cox (1990a,b)]. We have shown previously that stabilization of the open conformation requires either ATP or another nucleoside triphosphate cofactor with an S<sub>0.5</sub> value of approximately 100 μM or less (Menge & Bryant, 1992; Stole & Bryant, 1995). We are currently investigating the effect of alternate nucleoside triphosphate cofactors on the transient fluorescence of the [H163W]recA—ssDNA complex in order to elucidate the mechanistic basis for the dependence of the stability of the open conformation on the S<sub>0.5</sub> value of the nucleoside triphosphate cofactor.

The closed cycle portion of Scheme 4 represents the steady-state ATP hydrolysis cycle. All of the steps in this cycle are assumed to be in rapid equilibrium, and therefore all of the intermediates in this cycle can be treated, for kinetic purposes, as a single species. Because the saturation behavior that was observed for the amplitude of the ATP-mediated fluorescence change (Figure 3B) suggests that the isomerization of the complex from the closed to open conformation is reversible, the collected species represented by the steady-state hydrolysis cycle are depicted as being in equilibrium with the initial closed  $E_c \cdot \text{ATP}$  complex. In Scheme 4, we have arbitrarily shown the reversibility arising from a return of the  $E_o^* \cdot \text{ATP}$  species to the closed  $E_c \cdot \text{ATP}$  state, but because the closed cycle is in equilibrium, any of the species within the cycle could lead to the reversal. One possibility would be for the complex to collapse to a closed conformation at some point during the release of ADP and the rebinding of a new molecule of ATP. Since  $\text{ATP}\gamma\text{S}$  is not hydrolyzed appreciably on the time scale of the measurements and therefore does not readily lead to the formation an  $E \cdot \text{ADP}$  species, this would also account for the low reversibility of the  $\text{ATP}\gamma\text{S}$ -induced fluorescence change (Figure 5B).

Although our data indicate that the rate-determining step on the ssDNA-dependent ATP hydrolysis pathway is a pre-ATP hydrolysis isomerization of the recA–ssDNA complex and that this isomerization is accompanied (during the first turnover) by a transition of the recA–ssDNA complex from the closed to the open conformation, the exact mechanism of the closed to open transition is not clear. One possibility is that the transition occurs directly by a reorganization of the recA monomers on the ssDNA, with the monomers never leaving the DNA. A second possibility is that the pre-ATP hydrolysis isomerization may trigger a rapid dissociation of recA monomers (in the closed conformation) from ssDNA and a rapid reassembly of the monomers on the ssDNA (in the open conformation) before ATP hydrolysis begins; in this case, the rate of ATP hydrolysis during the first turnover would still be limited by the pre-ATP hydrolysis isomerization step. In either case, once the recA–ssDNA complex is in the open conformation, steady-state ATP hydrolysis continues via this complex at an observed turnover number of 18 min<sup>-1</sup>.

We emphasize that the polymeric recA–ssDNA filament is a complex system and that the kinetic models that are described in this report are undoubtedly oversimplifications. They do, however, provide a framework for developing more specific and detailed mechanistic models for the binding and hydrolysis of ATP by this complex. This, in turn, will provide a foundation for further studies directed toward

elucidating how ATP binding and hydrolysis are related to the binding of the second duplex DNA strand and the progression of the recA protein-mediated strand exchange reaction.

## REFERENCES

- Brenner, S. L., Mitchell, R. S., Morrical, S. W., Neuendorf, S. K., Schutte, B. C., & Cox, M. M. (1987) *J. Biol. Chem.* 262, 4011–4016.
- Bryant, F. R. (1988) *J. Biol. Chem.* 263, 8716–8723.
- Cox, M. M., & Lehman, I. R. (1981) *Proc. Nat. Acad. Sci. U.S.A.* 78, 3433–3437.
- Egelman, E. H. (1993) *Curr. Opin. Struct. Biol.* 3, 189–197.
- Kowalczykowski, S. C. (1991) *Annu. Rev. Biochem.* 20, 539–575.
- Lee, J. W., & Cox, M. M. (1990a) *Biochemistry* 29, 7666–7676.
- Lee, J. W., & Cox, M. M. (1990b) *Biochemistry* 29, 7677–7683.
- Menge, K. L., & Bryant, F. R. (1992) *Biochemistry* 31, 5151–5157.
- Roca, A. I., & Cox, M. M. (1990) *Crit. Rev. Biochem. Mol. Biol.* 25, 415–456.
- Stole, E., & Bryant, F. R. (1994) *J. Biol. Chem.* 269, 7919–7925.
- Stole, E., & Bryant, F. R. (1995) *J. Biol. Chem.* 270, 20322–20328.
- Story, R. M., Weber, I. T., & Steitz, T. A. (1992) *Nature* 355, 318–325.
- Weinstock, G. M., McEntee, K., & Lehman, I. R. (1979) *Proc. Nat. Acad. Sci. U.S.A.* 76, 126–130.
- Weinstock, G. M., McEntee, K., & Lehman, I. R. (1981) *J. Biol. Chem.* 256, 8850–8855.
- Yu, X., & Egelman, E. H. (1992) *J. Mol. Biol.* 225, 193–216.

BI962881L